fermentation

MDPI

Article

Integrated System of Microalgae Photobioreactor and Wine Fermenter: Growth Kinetics for Sustainable CO_2 Biocapture

María Carla Groff [1,2,3,*,†], Cecilia Fernández Puchol [2,3,†], Rocío Gil [1], Lina Paula Pedrozo [1], Santiago Albareti [3], Ana Belén Manzanares [1], Emilia Sánchez [3] and Gustavo Scaglia [2,3]

[1] Instituto de Biotecnología, Facultad de Ingeniería, Universidad Nacional de San Juan (IBT-FI-UNSJ), San Juan 5400, Argentina; rocio.mariel.gil@gmail.com (R.G.); paulapedrozo17@gmail.com (L.P.P.); anabelenmanzanares@gmail.com (A.B.M.)
[2] Consejo Nacional de Investigaciones Científicas y Técnicas (CONICET), Buenos Aires 1425, Argentina; mcfernandez@unsj.edu.ar (C.F.P.); gscaglia@unsj.edu.ar (G.S.)
[3] Instituto de Ingeniería Química, Facultad de Ingeniería, Universidad Nacional de San Juan (IIQ-FI-UNSJ), San Juan 5400, Argentina; salbareti@gmail.com (S.A.); emiliasoledad72@gmail.com (E.S.)
* Correspondence: mcarlagroff@gmail.com; Tel.: +54-9-264-543-6303
† These authors contributed equally to this work.

Abstract: Microalgae possess the remarkable ability to autotrophically grow, utilizing atmospheric carbon dioxide (CO_2) for photosynthesis, thereby converting solar energy into chemical energy and releasing oxygen. This capacity makes them an effective tool for mitigating industrial CO_2 emissions. Mathematical models are crucial for predicting microalgal growth kinetics and thus assessing their potential as industrial CO_2 sequestration agents under controlled conditions. This study innovatively evaluated the effect of continuously supplying CO_2 from winemaking processes on microalgal cultivation and biomass production, demonstrating a novel approach to both carbon capture and the valorization of a valuable by-product. To analyze microalgal growth kinetics, three mathematical models were employed: Logistic, First Order Plus Dead Time, and Second Order Plus Dead Time. Optimal parameter values for each model were identified using a hybrid search algorithm developed by our research group. First, an integrated microvinification system was established, utilizing two microalgae species, *Chlorella* spp. (FAUBA-17) and *Desmodesmus spinosus* (FAUBA-4), in conjunction with yeast fermenters. This system facilitated a comparison of the biomass kinetics of these two microalgae species, selecting *Chlorella* spp. (FAUBA-17) as the most suitable candidate for subsequent cultivation. A pilot-scale vertical column photobioreactor was then constructed and installed at the Casimiro Wines boutique winery in Angaco, San Juan, Argentina. After 15 days of operation within the photobioreactor, a biomass growth of 1.04 ± 0.05 g/L and 1.07 ± 0.1 g/L was obtained in Photobioreactors 1 and 2, respectively. This novel integrated approach to CO_2 capture in the winemaking process is unprecedented. These findings highlight the potential for producing high-value microalgal biomass, promoting the establishment of a local biorefinery and fostering a circular economy and sustainable social development.

Keywords: microalgae; winemaking; CO_2 biocapture; photobioreactor; growth kinetic

Academic Editor: Giuseppe Italo Francesco Perretti

Received: 23 December 2024
Revised: 23 January 2025
Accepted: 24 January 2025
Published: 28 January 2025

Citation: Groff, M.C.; Puchol, C.F.; Gil, R.; Pedrozo, L.P.; Albareti, S.; Manzanares, A.B.; Sánchez, E.; Scaglia, G. Integrated System of Microalgae Photobioreactor and Wine Fermenter: Growth Kinetics for Sustainable CO_2 Biocapture. *Fermentation* **2025**, *11*, 58. https://doi.org/10.3390/fermentation11020058

1. Introduction

The environmental impact of human activity is increasingly evident, as global CO_2 emissions from fossil fuels have risen by over 60% in the last 30 years. This has led to a 1.1 °C increase in the average global temperature compared to pre-industrial levels, making the period from 2016 to 2020 the warmest on record [1]. Addressing this issue requires

urgent action; global CO_2 emissions must decline by 7% annually until 2030 to meet climate targets. Agriculture and industrial activity are significant contributors to these emissions, together accounting for approximately 45% of global greenhouse gas emissions [2]. Transforming these sectors is therefore essential. Adopting sustainable practices grounded in bioeconomic principles presents a viable solution, as this can mitigate environmental impacts, conserve natural resources, and advance long-term global sustainability goals.

Microalgae represent a versatile and sustainable solution to pressing environmental challenges, particularly those associated with carbon emissions and resource depletion [3]. As some of the earliest photosynthetic organisms, microalgae exhibit exceptional rates of CO_2 conversion into biomass, significantly exceeding those of terrestrial plants [4]. Notably, microalgae can capture substantial amounts of CO_2, fixing 10 to 50 times more CO_2 than terrestrial plants while producing an average of 1.83 g of biomass per gram of CO_2 consumed [5]. This capability makes microalgae an effective tool for mitigating greenhouse gas emissions, particularly when cultivated on non-fertile lands using photobioreactors [4]. Furthermore, microalgae contribute to bioremediation by effectively retaining heavy metals and other pollutants [6,7]. Their biomass, rich in proteins, oils, and antioxidants, offers a valuable resource for various applications, including biofertilizer, biofuels, food production, and pharmaceuticals [8].

In San Juan, Argentina, the winemaking industry plays an important role in the regional economy, competing in international markets where sustainability is increasingly valued. However, the industry faces significant challenges in reducing its carbon footprint, as it is both energy-intensive and heavily reliant on conventional practices that contribute to global CO_2 emissions. While Argentina lacks specific legislation regulating CO_2 emissions from winemaking, calculating the carbon footprint offers a viable approach for quantification. This approach aligns with global green labeling standards, enabling wineries to enhance their competitiveness in international markets. By adopting these practices, San Juan could position itself as a leader in innovative and sustainable industrial solutions, setting an example for the global winemaking industry [9].

These challenges underscore the critical need to adopt sustainable solutions to mitigate the environmental impact of agro-industrial activities, particularly in light of increasing international attention to climate change [9]. The province boasts solar radiation intensity reaching up to 7.5 $kWh/m^2/day$ and between 4 and 9 h of sunlight daily, depending on the season and area [10]. Its vast expanses of non-arable desert and semidesert land provide ideal conditions for installing microalgae photobioreactors. By integrating such systems into local wineries, CO_2 emissions from wine fermentation, estimated at 14,400 tons for 2023, based on stoichiometric analysis [11] and official data from Instituto Nacional de Vitivinicultura (INV) [12], could be effectively captured, reducing the industry's carbon footprint. This approach not only addresses the immediate challenge of emissions reduction but also aligns with the concept of integrated biorefineries, where microalgae cultivation can generate high-value bioproducts alongside CO_2 capture [13].

The integration of microalgae cultivation and winemaking presents a compelling solution due to its ability to transform CO_2 emissions into valuable biomass, aligning with the principles of a circular economy. Leveraging local resources, such as high solar radiation and non-arable land, enhances the feasibility of this approach in regions like San Juan. Additionally, the biomass produced can generate high-value products such as biofertilizers, pigments, and food supplements, diversifying revenue streams for wineries. By adopting this strategy, wineries can significantly reduce their carbon footprint, improve their competitiveness in sustainability-conscious markets, and contribute to global efforts against climate change. The modular nature of microalgae cultivation systems also ensures scalability, making this integration accessible to wineries of various sizes.

Bioprocesses, like microalgae cultivation, are inherently complex due to their nonlinear dynamics and dependence on living organisms. These systems involve intricate interactions between multiple variables, including nutrient availability, light intensity, and CO_2 concentration, that fluctuate over time [14]. Furthermore, the sensitivity of microorganisms to environmental disturbances, along with the challenge of maintaining optimal conditions without inhibiting growth or causing cell death, highlights the need for precise control strategies [15]. Addressing these challenges requires advanced mathematical tools for modeling and optimization, enabling better predictions of system behavior and more efficient process management [16]. For instance, dynamic modeling, parametric identification, optimization, control, and state estimation have proven essential for scaling bioprocesses while maintaining high yields and quality [17], and enhancing the efficiency and reproducibility of biological systems [18–21].

Process engineering plays a crucial role in developing systematic methodologies for designing, modeling, scaling up, optimizing, and controlling these complex systems. The integration of process engineering with bioprocesses facilitates the development of innovative solutions, such as the use of photobioreactors for microalgae cultivation. Photobioreactors can be classified into open and closed types, with closed systems generally being more efficient because they offer better control over cultivation conditions, such as temperature and CO_2 concentration. However, they are also more expensive due to their advanced technologies and infrastructure [22,23]. These systems enhance the control of cultivation parameters and promote sustainability by enabling efficient CO_2 capture and biomass production. By combining engineering principles with biological processes, photobioreactor technology exemplifies the potential of multidisciplinary approaches to address global challenges such as climate change and resource scarcity.

This paper presents a comprehensive study integrating microalgae cultivation into the winemaking industry to mitigate CO_2 emissions. To achieve this, we developed an integrated system that utilizes a microalgae photobioreactor to capture the CO_2 released during grape must fermentation and produce microalgal biomass. Initially, a laboratory-scale microvinification process was conducted to select between two microalgae species based on their biomass kinetics. Subsequently, a pilot-scale column photobioreactor was constructed and installed at the Casimiro Wines boutique winery in Angaco, San Juan, Argentina. The fermentation of 150 L of white grape juice was carried out in a 300 L stainless steel tank. The photobioreactor was then coupled to the fermentation tank, enabling the biocapture of CO_2 from the fermenting must by the microalgae cells. Experimental data from these integrated systems were analyzed using three mathematical models, incorporating a novel hybrid parameter optimization technique for the most accurate fit.

Our findings demonstrate this innovative approach's potential to enhance sustainability in winemaking while contributing to CO_2 reduction efforts.

2. Materials and Methods

2.1. Microalgae Inoculum and Growth Conditions

The microalgae inoculum *Chlorella* spp. (FAUBA-17) and *Desmodesmus spinosus* (FAUBA-4) were obtained from the Colección de Cultivos de Microalgas, Facultad de Agronomía of Universidad Nacional de Buenos Aires (CCM-FAUBA), Argentina.

The cultivation of both strains was carried out using a modified Bold's Basal Medium (mBBM) prepared from concentrated stock solutions [24]. Each of these stock solutions was prepared by dissolving a weighed quantity of the nutrient in distilled water under constant agitation and then made up to the final volume with distilled water. To ensure microbiological sterility, the stock solutions were dispensed into screw-cap autoclavable Falcon tubes and autoclaved at 121 °C for 20 min. Refrigeration (4 °C) was used for short-

term storage (up to one month), while freezing (−20 °C) was employed for long-term preservation [24]. The mBBM (g/L) was composed of 1.5 mL $NaNO_3$ (170 g/L), 1.65 mL $CaCl_2$ (11.3 g/L), 3 mL $MgSO_4{\cdot}7H_2O$ (25 g/L), 10 mL K_2HPO_4 (7.5 g/L), 10 mL KH_2PO_4 (17.5 g/L), 1 mL NaCl (25 g/L), 1 drop of trace element stock solutions EDTA (50 g/L), $FeSO_4{\cdot}7H_2O$ (5 g/L), H_3BO_3 (11 g/L), and Bold trace metals stock solution ($ZnSO_4{\cdot}7H_2O$ (8.8 g/L), $MnSO_4.H_2O$ (1.4 g/L), $Na_2MoO_4{\cdot}2H_2O$ (1.2 g/L), $CuSO_4{\cdot}5H_2O$ (1.5 g/L), and $CoCl_2{\cdot}6H_2O$ (0.4 g/L)). The stock solutions were added to distilled water under aseptic conditions, ensuring the desired concentration in the mBBM medium. Prior to autoclaving at 121 °C for 20 min, the pH was adjusted to 7.0.

In total, 10 mL of each microalgae inoculum was grown in 250 mL flasks containing 100 mL of sterilized mBBM. The cultures were incubated for 10 days in a microbial culture room at a constant temperature of 24 °C with agitation in an orbital shaker at 120 rpm under a 12:12 (light/dark) photoperiod. The light intensity was maintained at 200 μmol/m^2.s (Apogee Instruments, MQ-500, Logan, UT, USA). To ensure culture quality, microalgae were routinely monitored microscopically and tested for bacterial contamination. Axenicity testing was performed by incubating 1 mL of culture in 9 mL of 1% glucose mBBM for 48 h, with turbidity indicating bacterial contamination (a detailed discussion of the results of this quality testing is beyond the scope of this study).

2.2. Biological Capture of CO_2 from Grape Must Fermentation by Microalgae at Lab Scale

First, lab-scale experiments were carried out to choose the faster-growing microalgae species based on their kinetics, and use it, afterwards, to enhance the performance of a pilot-scale unit at Casimiro Winery.

The fermentation assays were performed under static conditions in six Erlenmeyer flasks of 1 L containing 750 mL of sterile grape must (A1–A6 flasks, Figure 1). The grape must medium consisted of grape must, distillated water, nutrients (yeast extract, thiamine, and diammonium phosphate), and tartaric acid. As a result, the initial characteristics were as follows: 21 °Bx (the equivalent of 205 g/L of sugar), pH 3.4, total acidity 5.5 g/L, and easily assimilable nitrogen 220 mg/L [25]. It was inoculated with 2×10^6 cells/mL of commercial yeast strain Vin 13 (Anchor Oenology, France). Prior to inoculation, yeast was activated in 12 °Bx sterile grape must at 25 °C and 120 rpm for 24 h.

Two of the flasks (A1 and A2) where alcoholic fermentation took place were used as duplicates to monitor the daily weight loss, which corresponded to the release of CO_2, until a constant weight was reached.

A series of flasks, B1–B6 (see the middle series of flasks in Figure 1), were used to carry out the CO_2 fermentation from microalgae. The flasks were 250 mL in volume and contained 125 mL of mBBM with microalgae inoculum at a concentration of 1×10^6 cells/mL (X_0). The A3 and A4 flasks were connected to the B3 and B4 flasks containing *D. spinosus* (FAUBA-4), while the flasks A5 and A6 were connected to the B5 and B6 flasks containing *Chlorella* spp. (FAUBA-17). Moreover, the B1 and B2 flasks contained each of the two microalgae which were cultivated under atmospheric CO_2 (ambient air).

Microalgae samples were taken in duplicates every 24 h, determining the cell concentration using a Neubauer chamber. The experiment was carried out in a incubated room at 25 °C for 22 days. The B flasks were placed under agitation at 120 rpm and a 12:12 (light/dark) photoperiod with photosynthetic active radiation (PAR) of 200 μmol/m^2.s.

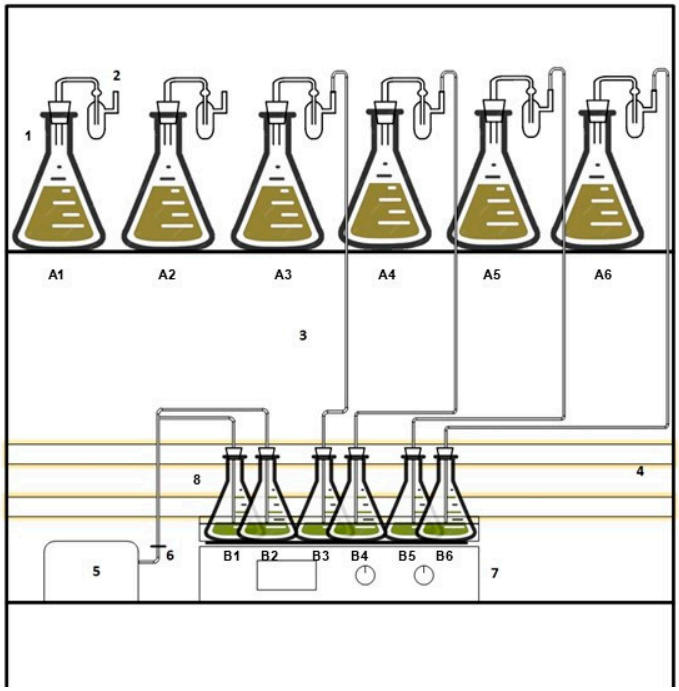

Figure 1. Integrated grape must fermentation and microalgae CO_2 biocapture system at laboratory scale. 1. Grape must fermentation (A1–A6 flasks); 2. Mueller valve; 3. CO_2 transport line; 4. 12 W cool white LED tubes; 5. 10 W air pump with 10 L/min flow rate 6. Air transport line with 50 mm vent filter (0.22 µm PTFE membrane); 7. Orbital shaker; 8. Microalgae cultures: B1–B2 flasks containing *Chlorella* spp. (FAUBA-17) and *D. spinosus* (FAUBA-4) which was cultivated under atmospheric CO_2 (ambient air); B3–B4 flasks containing *D. spinosus* (FAUBA-4); and B5–B6 flasks containing *Chlorella* spp. (FAUBA-17) aerated with the CO_2 fermentation.

2.3. Construction of a Pilot-Scale Tubular Photobioreactor and Integration with Fermentation Tank

As part of this study, an experimental pilot-scale CO_2 biocapture unit was constructed at the Instituto de Ingeniería Química (IIQ-FI-UNSJ). As depicted in Figure 2, this unit consisted of the following:

- Two vertical tubular photobioreactors, each measuring 400 mm in height and 150 mm in diameter (WP1: Winery Photobioreactor 1 and WP2: Winery Photobioreactor 2). The reactor body was fabricated from 1 mm thick polycarbonate sheets, while the top and bottom caps were made from 3 mm thick polycarbonate. For added structural integrity, 3 mm thick steel caps and threaded rods were incorporated. Each photobioreactor was equipped with: a sterile air/CO_2 mixture inlet; an airlock for gas outlet; a valve for sample collection; and ports for loading and unloading.
- The air distribution system comprised an air pump with a capacity of 110 L/min, a 50 mm diameter membrane filter (0.22 µm Teflon) for sterilizing the air/CO_2 mixture, 3/8″ hose, a T-junction to mix ambient air with CO_2 from the fermentation process, and valves to regulate the flow of the air/CO_2 mixture to each photobioreactor.
- The support structure consisted of 30 × 30 mm pipe frame and metal mesh, with an electrical panel and other electrical installations, loading/unloading pumps, and hoses with valves.
- The lighting system consisted of six 9 Watt LED fluorescent lights positioned equidistantly around each photobioreactor to ensure homogeneous light distribution. A 12:12 (light/dark) photoperiod was programmed.

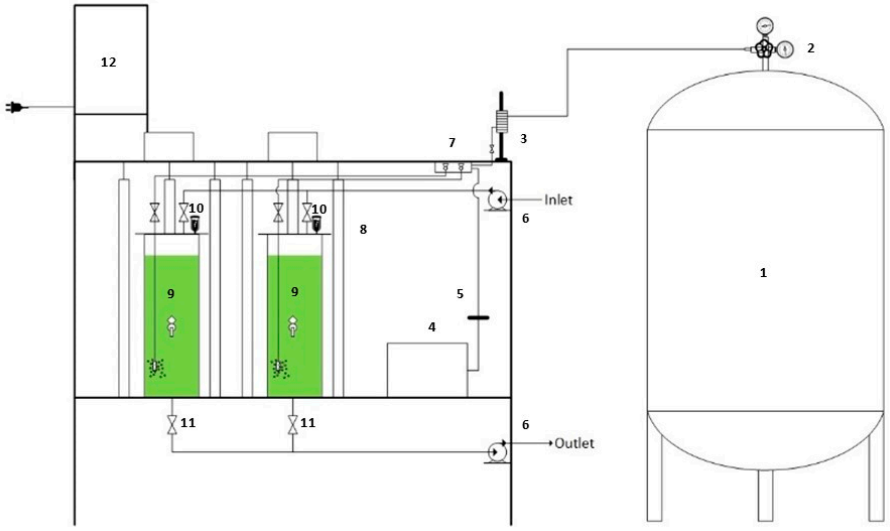

Figure 2. Integrated system of microalgae photobioreactor and wine fermenter installed at winery (pilot-scale). 1. Wine fermentation stainless steel tank; 2. Manometer; 3. CO_2 transport line and rotameter; 4. 35 W air pump with 110 L/min flow rate; 12 W cool white LED tubes; 5. Air transport line with 50 mm vent filter (0.22 µm PTFE membrane); 6. 27 W liquid transfer pump; 7. Air/CO_2 distributor; 8. 12 W cool white LED tubes; 9. Vertical tubular photobioreactors with *Chlorella* spp. (FAUBA-17) culture; 10. Airlock; 11. 1/2″ Full bore ball valve; 12. Main electrical panel.

The inoculum of the selected microalgae (1×10^7 cells/mL) and the sterile mBBM stock solutions were prepared at the IIQ.

The culture medium, inoculum, and photobioreactor were transported to Casimiro Wines Winery (Angaco, San Juan, Argentina). The cellar room was selected for installing the integrated system to capture CO_2 from wine fermentation due to its 18 °C temperature.

The sterile mBBM stock solutions were mixed with water to a final volume of 12 L. The final solution was sterilized by exposure to a UVC germicidal lamp for 20 min. The photobioreactor and pipes were sterilized with 0.2% peracetic acid and then filled with the mixture of culture medium and inoculum at 10% v/v ($X_0 = 1 \times 10^6$ cells/mL).

The photobioreactor was coupled to the 300 L wine fermentation tank with 150 L of white grape juice. The inoculum concentrations employed in the fermentation trials were 2×10^6 cells/mL. The same commercial yeast inoculum was used, at the same concentration, as in the microvinification trials. The focus of this study was not on defining the kinetics of fermentation. As such, the fermentation process was operated by winery personnel, with temperature and density (°Bé) monitored daily to control fermentation performance.

The microalgae bioprocess was carried out for 15 days in batch mode. Duplicate samples were collected daily to monitor pH and cell concentration (using a Neubauer chamber). The final total dry weight of the microalgal biomass was quantified by gravimetric analysis. Ten milliliters of the culture was filtered onto pre-weighed glass fiber filters (pore size 1.2 µm). The filters were then washed with distilled water and dried in oven at 80 °C for 24 h until reaching a constant weight. The dry biomass of microalgae per unit of volume (g/L) was calculated by the difference between the dry weight of the glass fiber filters plus the dry biomass and the tare of the dry membrane, and then dividing this difference by the sample volume [26].

2.4. Kinetic Modeling and Parametric Identification of CO_2 Biocapturing Microalgae

With experimental data obtained from samples collected during laboratory-scale microvinification and pilot-scale winery fermentation, growth curves were developed and fitted to three mathematical models: the Logistic Model, the First Order Plus Dead Time

Model (FOPDT), and the Second Order Plus Dead Time Model (SOPDT). A brief description of each model is provided below:

- Logistic Model (LM): Also known as the logistic equation, this differential equation is used to describe population growth within a limited environment [27]. Equation (1) presents the standard form of the logistic equation:

$$\frac{dX}{dt} = \mu_{max}\left(1 - \frac{X}{X_{max}}\right)X;\ \mathrm{X}(0) = \mathrm{X}_0 \tag{1}$$

where dX/dt is the rate of change in microalgae population over time [g/L.day], μ_{max} denotes the intrinsic growth rate of the microalgae population [1/day], X represents the microalgae population as a function of time [g/L or cells/L], X_{max} is the maximum microalgae population the environment can sustain [g/L or cells/L], and X_0 is the initial population at time t = 0 [g/L or cells/L]. This equation captures how population growth slows as it approaches environmental limits, culminating in equilibrium. The general solution to this differential equation is

$$X(t) = \frac{X_{max}}{1 + \left(\frac{X_{max}}{X_0} - 1\right) exp^{-\mu_{max}\ .t}} \tag{2}$$

This model is recognized for its robust fit to microbial growth data and has been extensively employed in bioprocesses since its inception. It continues to be a cornerstone model in numerous studies [28–30].

- FOPDT: This type of mathematical model describes the dynamic response of a system using a first-order linear differential equation combined with a delay term [31]. These models are widely employed to describe dynamic systems in engineering and process control, particularly in contexts involving system inertia or response delays. Equation (3) shows the differential equation for this [32]:

$$\frac{dX}{dt} + \frac{X}{T_p} = \frac{1}{T_p}X_{max}(t - T_0),\ X(0) = X_0 \tag{3}$$

where the function $X_{max}(t - T_0)$ is defined by

$$X_{max}(t - T_0) = \begin{cases} X_{max}\ \ for\ t \geq T_0 \\ X_0\ for\ t < T_0 \end{cases} \tag{4}$$

This model has two parameters of time: T_p is the system time constant, which determines the speed of the system's response [day], and T_0 is the delay in the system input [day].

- SOPDT: The general description is similar to FOPDT, with the difference that this model is represented by a second-order linear differential equation with a delay term [31]. The SOPDT general form is shown in Equation (5):

$$\frac{d^2X}{dt^2} + \left(\frac{1}{T_{p_1}} + \frac{1}{T_{p_2}}\right)\frac{dX}{dt} + \frac{X}{T_{p_1}T_{p_2}} = \frac{1}{T_{p_1}T_{p_2}}X_{max}(t - T_0),\ X(0) = X_0\ ,\ \frac{dX}{dt}(0) = 0 \tag{5}$$

where the function $X_{max}(t - T_0)$ is defined by Equation (4), where d^2X/dt^2 is the second derivative of the output variable with respect to time [g/L.day^2], and where T_{p1} and T_{p2} are constant of time of the system [day]. Selecting appropriate parameters (T_{p1}, T_{p2}, X_{max}, and T_0) is essential to accurately capture the system's real behavior.

Once the three mathematical models have been defined, it is necessary to quantify how well each model fits the experimental data. This is typically performed by calculating goodness-of-fit statistics such as the coefficient of determination (R^2). An R^2 value approaching 1 signifies that the regression model provides a very good fit to the data, explaining a substantial portion of the variance in the dependent variable. A value of R^2 close to zero reveals that the proposed model has a poor fit to the data, making it insufficient for accurate predictions [33].

The optimal value for each parameter for each model (X_{max}, μ_{max}, T_p T_{p1}, T_{p2}, and T_0) was determined by applying a hybrid search algorithm developed by our research group [18]. This parametric identification method combines two widely used techniques: the Monte Carlo Algorithm [34] and the Genetic Algorithm [35]. The hybrid approach leverages the exploratory nature of Monte Carlo sampling and the optimization capabilities of Genetic Algorithms, combining their strengths to achieve robust parameter estimation. The statement of the optimization problem consists of finding the best value of the mathematical model's parameters that maximizes the performance index, J, which is equal to R^2:

$$\underset{[X_{max},\ \mu_{max},\ T_p,\ T_{p1},\ T_{p2},\ T_0]}{max\ J} = R^2 \quad (6)$$

subject to Equation (2) to Equation (5).

Figure 3 illustrates the proposed hybrid algorithm, outlining the sequence and interplay between the Monte Carlo and Genetic Algorithm components.

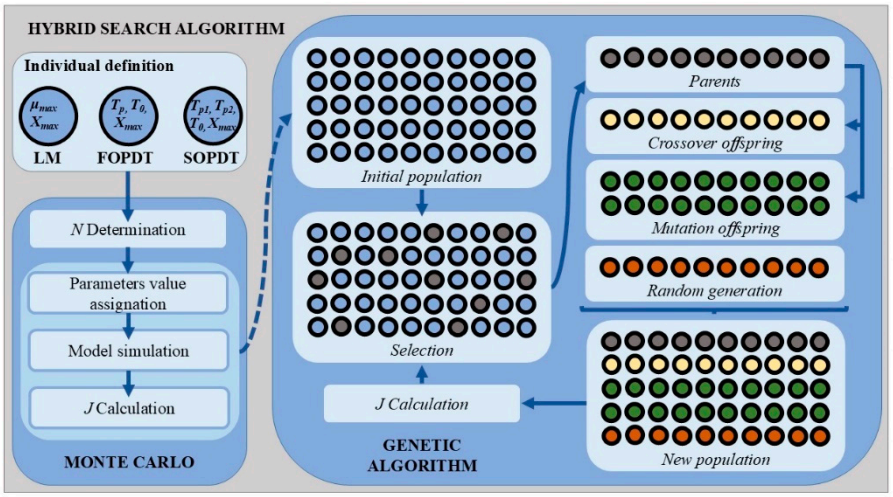

Figure 3. Hybrid search algorithm sequence applied in this study. Monte Carlo Steps: 1. Define the parameters to search, forming a vector called "individual"; 2. Determine the number of simulations N = 100; 3. Assign random values to each parameter within a typical observed range; 4. Substitute experimental X values and randomly assigned parameters into the respective model; 5. Calculate J; 6. Repeat Steps 3 to 5 until N iterations are completed. Genetic Algorithm Steps: 1. Selection: Starting with the Monte Carlo-generated population (100 individuals), the top 20 individuals with the best J values are selected to form the "parents" for the first generation; 2. Crossover: Here, 20 offspring are produced by randomly selecting pairs from the parent set and performing single-point crossover on random parameter positions; 3. Mutation: At this point, 40 mutations occur by selecting a random individual and altering one random parameter; 4. Diversification: To prevent local maxima, 20 new random individuals are generated, as in Monte Carlo; 5. New Generation: The new population includes 20 parents, 20 offspring from crossover, 40 from mutation, and 20 random individuals; 6. Iteration: With 100 individuals in the new generation, J is calculated for each, and the process (Steps 1–6) is repeated for L = 10 generations.

This visual representation clarifies the algorithm's design and optimization workflow. This layout helps to visualize the flow from initial random sampling, through iterative optimization steps like crossover and mutation, to the final selection process, allowing for a comprehensive understanding of the algorithm's design and intended functionality.

The software Matlab R2015a was used to test the fit of the mathematical models for the microalgae kinetic growth.

3. Results and Discussion

3.1. Experimental Data, Mathematical Modeling, and Parametric Identification of Biological Capture of CO_2 at Laboratory Scale

According to the alcohol fermentation reaction (Equation (7)), 180 g of glucose is converted to 88 g of CO_2 or 44.8 L of CO_2 under standard temperature and pressure (STP) conditions (0 °C and 760 mmHg):

$$C_6H_{12}O_6 \rightarrow 2C_2H_5OH + 2CO_2 + \text{energy} \quad (7)$$

Since 1 L of grape must medium contained 205 g of glucose equivalent sugars, the volume of CO_2 anticipated to be produced from the complete conversion of sugars was 51 L. Consequently, the fermentation of 750 mL of grape must can potentially yield up to 38 L of CO_2 or 74 g of CO_2 (theoretical yield of CO_2). Figure 4 shows the accumulated CO_2 obtained in the microvinification assay.

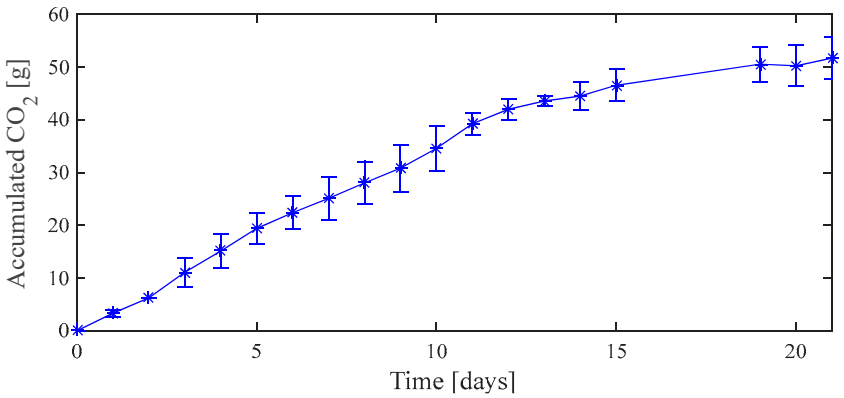

Figure 4. Production of CO_2 generated in the microvinification at laboratory scale.

The maximum CO_2 yield obtained in the assay, which peaked on day 21, was determined to be an average of 51.7 g (experimental or real yield of CO_2). This experimental yield represents 70% of the theoretical yield, a value lower than expected for several reasons:

- As a biological process, alcoholic fermentation is not the sole metabolic reaction; it is often accompanied by other biological reactions leading to the production of various metabolites, including glycerol, acetaldehyde, acetate, higher alcohols, esters, and hydrogen sulfide [36];
- Furthermore, the gaseous nature of CO_2 makes it challenging to measure without experiencing some loss, leading to underestimations in the gravimetric measurement.
- Finally, regarding the environmental conditions of the experiment, a constant room temperature of 25 °C was maintained, under which both wine fermentation and microalgal growth occurred. This temperature was chosen to prioritize optimal microalgal growth, as yeasts can function adequately at this temperature, although typical fermentation temperatures for white grape must range from 12 to 16 °C, which would result in a substantial reduction in microalgal growth rates. In larger installations, wine fermentation tanks are usually equipped with cooling jackets. This

technology allows for independent thermal control of the must, unlike the photobioreactor, whose operation is directly influenced by environmental conditions (such as light and temperature).

In general terms, microalgal growth and CO_2 utilization are constrained when CO_2 concentrations in the aeration gas fall below 0.5% due to low solubility in water and limited affinity of carbon fixation enzymes. Conversely, excessively high CO_2 levels (above 6–12%) can also impede growth by disrupting the carbon concentrating mechanism, which is essential for converting dissolved CO_2 into the more readily utilizable bicarbonate (HCO_3^-) [37].

Analysis of Figure 4 indicates three distinct phases characterized by varying CO_2 production rates: a rapid initial phase (days 1–5) with an average of 4.1 g CO_2/day, followed by a moderate phase (days 6–12) with 3.3 g CO_2/day, and a final phase (days 13–21) with a lower rate of 1.80 g CO_2/day. These findings underscore the adaptability of microalgae to dynamic CO_2 regimes. While this flexibility is advantageous for integrated bioprocesses, a more precise control of CO_2 supply could be achieved through pressurized gas storage [38]. Given that CO_2 capture and pressurization can result in substantial capital and operational expenses, this aspect is beyond the scope of this study.

Whereas previous research has emphasized the importance of gradual acclimation to low CO_2 concentrations (1.1% and 3.3%) for improving microalgal tolerance [39], our study adopted a unique approach. By mimicking the dynamic CO_2 production of wine fermentation, which resulted in a positive impact on the kinetic parameters compared to cultures that were aerated with air not containing CO_2 from fermentation (see Figure 5 and Table 1), this novel strategy challenges conventional acclimation protocols and offers new insights into microalgal responses to varying CO_2 conditions.

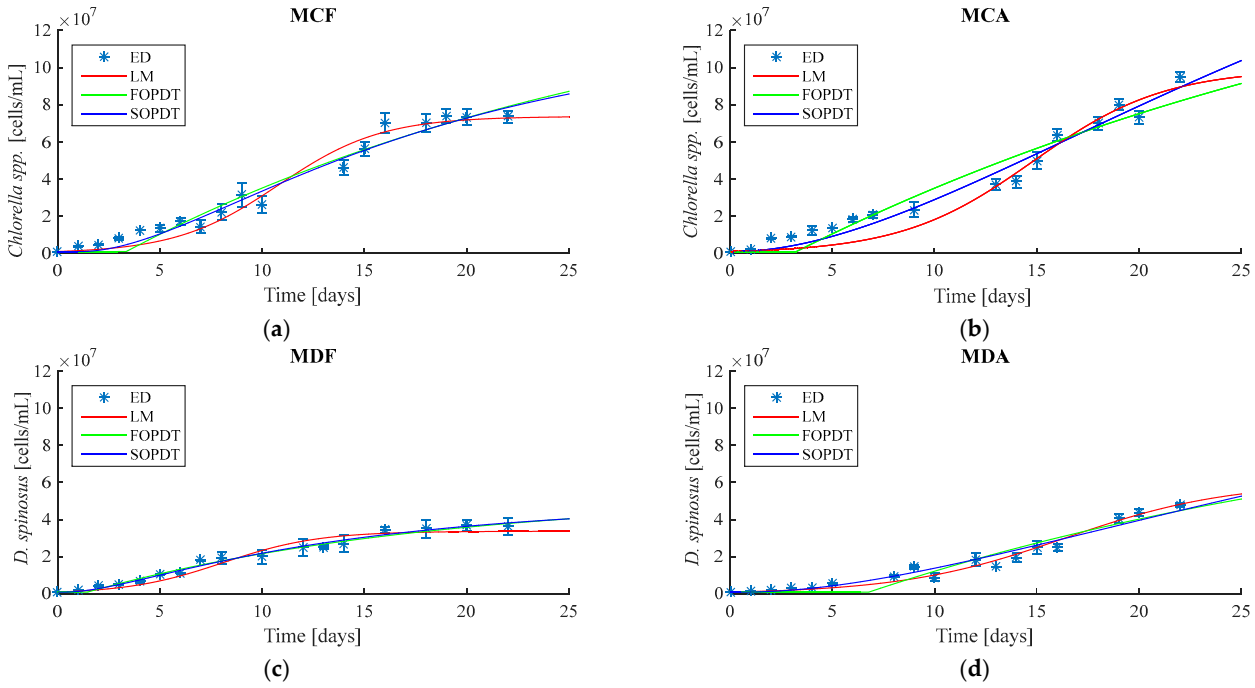

Figure 5. Comparison between the experimental data and mathematical models for microalgae cell growth kinetics. (**a**) MCF: Microvinification—*Chlorella* spp. aerated with CO_2 from fermentation; (**b**) MCA: Microvinification—*Chlorella* spp. aerated with atmospheric CO_2; (**c**) MDF: Microvinification—*D. spinosus* aerated with CO_2 from fermentation; and (**d**) MDA: Microvinification—*D. spinosus* aerated with atmospheric CO_2.

Table 1. Parameters determined by the hybrid optimization algorithm.

Scale	Culture	Mathematical Model's Parameters											
		Logistic Model			FOPDT Model				SOPDT Model				
		X_{max}	μ_{max}	R^2	X_{max}	T_p	T_0	R^2	X_{max}	T_{p1}	T_{p2}	T_0	R^2
LAB	**MCA**	9.93×10^7	0.31	0.944	2.00×10^8	36.07	3.25	0.942	2.31×10^8	15.82	17.07	0.18	0.969
	MCF	7.37×10^7	0.40	0.963	1.55×10^8	26.79	3.36	0.963	1.17×10^8	4.48	14.52	1.12	0.972
	MDA	6.01×10^7	0.25	0.974	1.08×10^8	29.36	6.79	0.940	1.31×10^8	21.57	14.69	0.61	0.961
	MDF	3.37×10^7	0.43	0.942	5.31×10^7	17.27	1.46	0.983	4.81×10^7	13.04	2.11	0.29	0.983
PILOT	**WP1**	1.08×10^7	0.56	0.921	1.30×10^7	7.83	0.70	0.982	1.00×10^7	1.81	2.42	0.74	0.983
	WP2	1.07×10^7	0.56	0.988	1.51×10^7	10.32	1.61	0.953	1.20×10^7	5.47	1.61	1.13	0.972

While alcoholic fermentation primarily produces CO_2 and ethanol, it also generates a range of volatile organic compounds (VOCs) in small quantities, including higher alcohols, organic acids, esters, aldehydes, and ketones. These compounds contribute to the sensory quality of fermented beverages [40]. Previous studies have demonstrated that certain microalgae species, such as *Scenedesmus* sp. and *Chlorella vulgaris*, can utilize organic acids like acetate as carbon sources, leading to increased biomass yield [41–43]. This suggests that certain VOCs generated during alcoholic fermentation could be sustainably used to enhance microalgae cultivation. No evidence has been found to suggest that VOCs inhibit microalgal growth.

The experimental data obtained from the laboratory-scale microvinification and winery photobioreactor trials enabled the construction of cell growth curves for *Chlorella* spp. (FAUBA-17) and *D. spinosus* (FAUBA-4). The microvinification tests were designed to evaluate the growth performance of these microalgae species using fermentation-derived CO_2 from grape must. *Chlorella* spp. (FAUBA-17) demonstrated superior growth under these conditions and was subsequently selected for pilot-scale CO_2 capture in the winery photobioreactors.

Growth curves from both the microvinification and winery-scale experiments were used to fit three mathematical models: LM, FOPDT, and SOPDT, as can be seen in Figure 5).

The hybrid optimization algorithm determined the parameters for each model, as summarized in Table 1.

During the microvinification trials, the behavior of *Chlorella* spp. (FAUBA-17) and *D. spinosus* (FAUBA-4) differed markedly. *Chlorella* spp. (FAUBA-17) showed enhanced growth with fermentation-derived CO_2 compared to atmospheric CO_2, as evidenced by higher values of X_{max} and μ_{max}. These results confirm its suitability for integration into winery processes at pilot scale. In contrast, *D. spinosus* (FAUBA-4) exhibited robust but less pronounced growth across both conditions, with lower X_{max} and μ_{max} values compared to *Chlorella* spp. (FAUBA-17). Such variation can be ascribed to the differential tolerance of various microalgal species to varying CO_2 concentrations [44], as well as to the different mechanisms by which each species absorbs atmospheric CO_2 [45]. *Chlorella* species are effective at capturing CO_2 and are particularly noteworthy for their high efficiency in converting elevated CO_2 levels into substantial biomass [46], as demonstrated in [47], where they showed that *Chlorella* had a capacity for a maximum CO_2 uptake rate of 0.412 g/L per day, with a daily CO_2 utilization reaching a maximum of 8.125 L. Regarding the use of *D. spinosus* as an efficient CO_2 capturer, species closely related to *Desmodesmus* and *Scenedesmus* have demonstrated high tolerance to elevated CO_2 levels, thriving at 15–20% CO_2 with biomass production reaching 0.67–1.11 g/L [48]. Our findings are consistent with previous research, which has established *Chlorella* as a microalga with a high tolerance for elevated CO_2 levels. This, in turn, positions *Chlorella* as a promising candidate for mitigating industrial CO_2 emissions.

3.2. Experimental Data, Mathematical Modeling, and Parametric Identification of Biological Capture of CO_2 from Fermentation Tank at Pilot Scale

The alcoholic fermentation, monitored by operators, started at 12.1 °Bé (equivalent to 217 g/L of sugar) and ended at 5.4 °Bé (80 g/L of sugar) [49], resulting in a yeast consumption of 137 g/L of sugar. Based on the stoichiometry of alcoholic fermentation (Equation (7)), where two moles of CO_2 are produced for each mole of glucose consumed, and considering the molar masses of glucose (180 g/mol) and CO_2 (44 g/mol), an estimated 66.97 g of CO_2 was produced per liter of grape must. Theoretically, the fermentation of 150 L of grape must would yield 10,050 g CO_2. However, considering a practical yield of 70%, as observed in microvinification, a production of 7840 g CO_2 was estimated.

As shown in Figure 2, this gas generated during fermentation was directed to two photobioreactors containing microalgae. Over a 15-day period, each photobioreactor received a total of 3920 g or 1983 L of CO_2.

One way to understand the behavior of CO_2 from grape must fermentation in the photobioreactors is through pH measurement, as it reflects its availability in the culture, i.e., which inorganic carbon species in the bicarbonate buffer system ($CO_{2(g)}$, HCO_3^- or CO_3^{2-}) predominates [4]. The pH range of the reactor cultures fluctuated between 7 and 7.4, a range where there is an equilibrium between HCO_3^- and $CO_{2(g)}$ species [50]. This clearly shows that the large contribution of CO_2 from fermentation was rapidly metabolized by the microalgae, since no marked decrease in pH was observed, as would be expected if the HCO_3^- ion accumulated. During the final fermentation stage, as CO_2 levels from the wine fermenter decreased, the pH remained stable between 7.2 and 7.4. Notably, this decline in CO_2 did not adversely affect the growth of *Chlorella* spp.

The experimental data obtained from the photobioreactor pilot scale in winery enabled the construction of cell growth curves for *Chlorella* spp. (FAUBA-17) (see Figure 6).

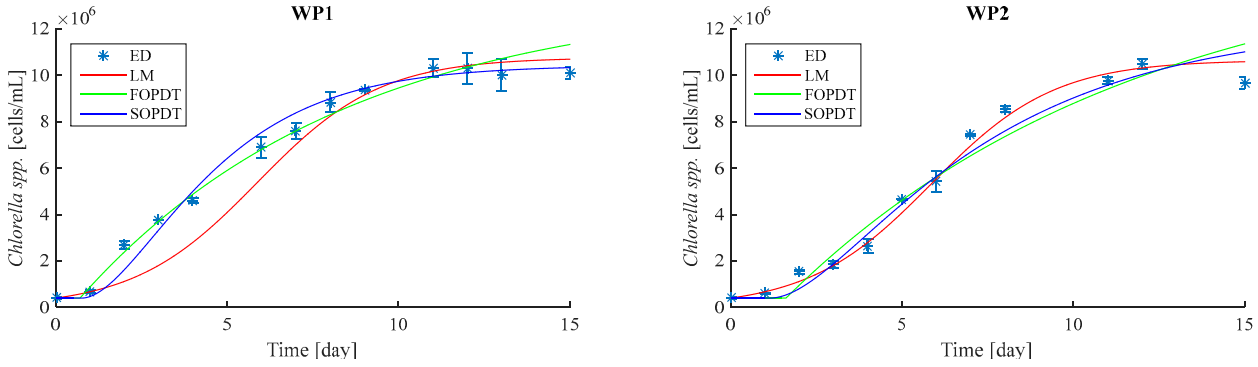

Figure 6. Experimental data of microalgae concentration compared to the model fit (WP1: Photobioreactor 1; WP2: Photobioreactor 2).

At the winery scale, two independent photobioreactors were used for *Chlorella* spp. (FAUBA-17) cultivation with fermentation-derived CO_2. The growth curves from each reactor were analyzed separately, and their corresponding parameters were fitted to the models (see Table 1). The results revealed a high degree of consistency between the reactors, with similar values for key parameters such as X_{max} and μ_{max}. This agreement demonstrates the reproducibility of the cultivation process under the tested conditions, further validating the reliability of the experimental setup and the accuracy of the applied mathematical models.

Analyzing the parameters in Table 1, all three models provided a good fit to the experimental data, as reflected in the consistently high R^2 values across all conditions. However, in most cases, the SOPDT model demonstrated superior performance, achieving

the highest R^2 values. This indicates its enhanced ability to capture both transient dynamics and steady-state behavior with greater accuracy. Figure 6 illustrates the experimental and modeled curves, showcasing the SOPDT model's effectiveness in closely representing the observed trends.

At the end of the experiment, an average biomass growth of 1.04 ± 0.05 g/L and 1.07 ± 0.1 g/L was recorded in Photobioreactors 1 and 2, respectively. These values fall within the range reported in other studies of CO_2 biocapture using microalgae such as *Chlorella vulgaris* (1 g/L) [11] and *Dunaliella tertiolecta* (1.10 ± 0.05 g/L) [5]. The results obtained in our pilot-scale study support the feasibility of this technology for carbon fixation.

Excessive water evaporation represents a limitation in the performance of the vertical column photobioreactor. The resulting solute concentration can cause osmotic stress in the microalgae and negatively affect photosynthetic growth rates [51]. To address this, a humidification column could be integrated to maintain optimal humidity levels within the reactor.

A simple-to-operate and versatile photobioreactor was successfully constructed, offering boutique wineries in San Juan a practical solution for reducing their carbon footprint and enabling the production of more sustainable wines.

The current literature highlights the potential of microalgae for mitigating wine industry emissions and utilizing by-products [52]. While research has explored using winery wastewater for microalgal cultivation [53–55] and sustainable wastewater treatment technologies [56], the integration of fermentation gases, such as CO_2, directly into microalgal cultivation systems has been largely unexplored. Previous studies have focused on alternative uses for captured fermentation gases, such as carbonated beverage production [38], rather than utilizing them for microalgal growth. Our study is pioneering in this integration, proposing an innovative approach that combines CO_2 capture from alcoholic fermentation with microalgae cultivation, contributing not only to the mitigation of greenhouse gas emissions but also to the generation of valuable biomass for industrial applications.

The results of this study demonstrated that combining photobioreactors with yeast fermentation provides a sustainable solution for capturing the CO_2 emitted during wine production. This approach enables microalgae cultivation, converting CO_2 into valuable biomass for the food, pharmaceutical, and cosmetic industries, contributing to climate change mitigation.

4. Conclusions

This study highlights *Chlorella* spp. (FAUBA-17) as a promising candidate for CO_2 capture in winery settings due to its enhanced growth performance with fermentation-derived CO_2, compared to *D. spinosus* (FAUBA-4). The reproducibility of cultivation in winery-scale photobioreactors and the robust fit of growth data to the SOPDT model underscore the reliability and precision of the experimental setup. These findings emphasize the importance of selecting appropriate models to accurately describe microalgal growth. While simpler models can offer a general understanding, the SOPDT linear model excels in providing detailed dynamic characterization, particularly valuable in complex systems. This capability is critical for optimizing CO_2 capture processes in winery settings, enabling more efficient integration of microalgae-based technologies into industrial operations and contributing to sustainability goals by reducing carbon emissions.

The mathematical models and hybrid optimization algorithm presented in this work offer a versatile framework for analyzing and predicting dynamic behavior in bioprocesses. Their application is not limited to winemaking but can be extended to other fermentation processes, bioreactors, and industrial scenarios where accurate growth modeling and

parameter estimation are fundamental. By improving model accuracy and parameter optimization, this approach can enhance process efficiency, reduce experimental costs, and support the design of scalable systems in the biotechnology and food industries. Furthermore, the potential economic savings and environmental benefits of adopting such integrated systems underscore their relevance for industrial operations aiming to reduce their carbon footprint.

For future work, we aim to continue developing our pilot-scale photobioreactor to increase its capacity and optimize energy consumption. We also plan to isolate native microalgae from San Juan and cultivate them in the photobioreactor, taking advantage of their adaptation to local conditions and improving yields. Additionally, efforts will focus on developing advanced control systems and exploring the integration of renewable energy sources, such as solar power, to further enhance the sustainability of the system.

Finally, this study emphasizes the importance of interdisciplinary collaboration between scientists, engineers, and entrepreneurs to address the technical and economic challenges associated with scaling up these technologies. Facilitating knowledge transfer and innovation in the industry across disciplines will be key to overcoming barriers to adoption and fostering widespread implementation of microalgae-based solutions in the industry.

Author Contributions: Conceptualization, M.C.G., C.F.P. and G.S.; methodology, M.C.G., R.G., L.P.P., A.B.M., S.A. and E.S.; software, G.S. and C.F.P.; formal analysis, M.C.G., G.S. and C.F.P.; investigation, M.C.G., R.G. and L.P.P.; writing—original draft preparation, M.C.G. and C.F.P.; writing—review and editing, M.C.G., C.F.P. and G.S.; supervision, G.S. All authors have read and agreed to the published version of the manuscript.

Funding: This article was financially supported by Universidad Nacional de San Juan (PDTS 2023–2024: 800202202000090SJ; CICITCA 2023–2024: 800202201001685J and 800202201001645J), CONICET (PIP 2022: 11220210100272CO), Secretaría de Ciencia, Tecnología e Innovación (PIPE 2022–2024: 1400-000119-2022 and 1400-000128-2022), and Fundación del Banco San Juan (Iniciativas Sustentables 2022).

Institutional Review Board Statement: This article does not contain studies with human participants or animals performed by any of the authors.

Informed Consent Statement: Informed consent was obtained from all individual participants included in the study.

Data Availability Statement: The original contributions presented in this study are included in the article. Further inquiries can be directed to the corresponding author.

Acknowledgments: The authors would like to express their sincere gratitude to "Casimiro Wines", and especially to their oenologist, Emiliano Lorenzo, for his active participation and unwavering support throughout this research. Likewise, the authors would also like to acknowledge the financial support provided by the Consejo Nacional de Investigaciones Científicas y Técnicas de Argentina (CONICET), the Universidad Nacional de San Juan (UNSJ), and the Fundación del Banco San Juan. During the preparation of this work, the authors used Gemini in order to improve readability and language. After using this tool, the authors reviewed and edited the content as needed and take full responsibility for the content of the publication.

Conflicts of Interest: The authors declare no conflicts of interest.

References

1. Kikstra, J.S.; Nicholls, Z.R.J.; Smith, C.J.; Lewis, J.; Lamboll, R.D.; Byers, E.; Sandstad, M.; Meinshausen, M.; Gidden, M.J.; Rogelj, J.; et al. The IPCC Sixth Assessment Report WGIII Climate Assessment of Mitigation Pathways: From Emissions to Global Temperatures. *Geosci. Model Dev.* **2022**, *15*, 9075–9109. [CrossRef]
2. Ritchie, H.; Rosado, P.; Roser, M. CO2 and Greenhouse Gas Emissions. Available online: https://ourworldindata.org/co2-and-greenhouse-gas-emissions (accessed on 12 September 2024).
3. Muñoz, R.; Fernandez Gonzalez, C. *Microalgae-Based Biofuels and Bioproducts: From Feedstock Cultivation to End-Products*; Elsevier Science: Amsterdam, The Netherlands, 2017; ISBN 9780081010273.
4. Jacob-Lopes, E.; Maroneze, M.M.; Queiroz, M.I.; Zepka, L.Q. *Handbook of Microalgae Based Processes and Products: Fundamentals and Advances in Energy, Food, Feed, Fertilizer, and Bioactive Compounds*; Elsevier: Amsterdam, The Netherlands, 2020; Volume 11, ISBN 978-0-12-818536-0.
5. Chagas, A.L.; Rios, A.O.; Jarenkow, A.; Marcílio, N.R.; Ayub, M.A.Z.; Rech, R. Production of Carotenoids and Lipids by *Dunaliella Tertiolecta* Using CO_2 from Beer Fermentation. *Process Biochem.* **2015**, *50*, 981–988. [CrossRef]
6. Murwanashyaka, T.; Shen, L.; Yang, Z.; Chang, J.S.; Manirafasha, E.; Ndikubwimana, T.; Chen, C.; Lu, Y. Kinetic Modelling of Heterotrophic Microalgae Culture in Wastewater: Storage Molecule Generation and Pollutants Mitigation. *Biochem. Eng. J.* **2020**, *157*, 107523. [CrossRef]
7. Tang, D.Y.Y.; Khoo, K.S.; Chew, K.W.; Tao, Y.; Ho, S.H.; Show, P.L. Potential Utilization of Bioproducts from Microalgae for the Quality Enhancement of Natural Products. *Bioresour. Technol.* **2020**, *304*, 122997. [CrossRef] [PubMed]
8. Jacob, A.; Ashok, B. Potential of Amyl Alcohol Mixtures Derived from *Scenedesmus Quadricauda* Microalgae Biomass as Third Generation Bioenergy for Compression Ignition Engine Applications Using Multivariate-Desirability Analysis. *Energy Sources Part A Recover. Util. Environ. Eff.* **2021**, *4*, 8542–8553. [CrossRef]
9. Wang, S.; Mukhambet, Y.; Esakkimuthu, S.; Abomohra, A.E.F. Integrated Microalgal Biorefinery–Routes, Energy, Economic and Environmental Perspectives. *J. Clean. Prod.* **2022**, *348*, 131245. [CrossRef]
10. Miguel Montenegro San Juan y Su Politica de Desarrollo de La Energia Fotovoltaica. Available online: https://sisanjuan.gob.ar/interes-general/2019-10-17/18102-san-juan-y-su-politica-de-desarrollo-de-la-energia-fotovoltaica (accessed on 10 December 2024).
11. D'Alberti, V.; Cammalleri, I.; Bella, S.; Ragusa, M.; Pavan, M.; Ragusa, R. Production of Algae with CO_2 from Wine Fermentation: An Important Way to Reduce Emissions. In Proceedings of the 23rd European Biomass Conference and Exhibition, Vienna, Austria, 1–4 June 2015; pp. 238–244. [CrossRef]
12. INV. *Informe Anual de Cosecha y Elaboración 2023*; Instituto Nacional de Vitivinicultura: Mendoza, Argentina, 2023; pp. 1–81.
13. Xu, S.; Jiang, Y.; Liu, Y.; Esakkimuthu, S.; Chen, H.; Wang, S. Impact of Constant Magnetic Field on Enhancing the Microalgal Biomass and Biomolecules Accumulations and Life Cycle Assessment of the Approach. *Algal Res.* **2024**, *80*, 103563. [CrossRef]
14. Guzmán, J.L.; Acién, F.G.; Berenguel, M. Modelado y Control de La Producción de Microalgas En Fotobiorreactores Industriales. *Rev. Iberoam. De Automática E Informática Ind.* **2020**, *18*, 1. [CrossRef]
15. Ochoa, S. A New Approach for Finding Smooth Optimal Feeding Profiles in Fed-Batch Fermentations. *Biochem. Eng. J.* **2016**, *105*, 177–188. [CrossRef]
16. Allampalli, S.S.P.; Sivaprakasam, S. Unveiling the Potential of Specific Growth Rate Control in Fed-Batch Fermentation: Bridging the Gap between Product Quantity and Quality. *World J. Microbiol. Biotechnol.* **2024**, *40*, 196. [CrossRef] [PubMed]
17. Zhang, X.; Zhao, J.; Zhang, J.; Su, S.; Huang, L.; Ye, J. Kinetic Modelling of Microalgal Growth and Fucoxanthin Synthesis in Photobioreactor. *Int. J. Chem. React. Eng.* **2022**, *20*, 723–734. [CrossRef]
18. Fernández, C.; Pantano, N.; Godoy, S.; Serrano, E.; Scaglia, G. Optimización de Parámetros Utilizando Los Métodos de Monte Carlo y Algoritmos Evolutivos. Aplicación a Un Controlador de Seguimiento de Trayectoria En Sistemas No Lineales. *Rev. Iberoam. Automática E Informática Ind.* **2018**, *16*, 89–99. [CrossRef]
19. Pantano, M.N.; Fernández, M.C.; Ortiz, O.A.; Scaglia, G.J.E.; Vega, J.R. A Fourier-Based Control Vector Parameterization for the Optimization of Nonlinear Dynamic Processes with a Finite Terminal Time. *Comput. Chem. Eng.* **2020**, *134*, 106721. [CrossRef]
20. Fernandez, C.; Pantano, N.; Rodriguez, L.; Scaglia, G. Additive Uncertainty Consideration for Nonlinear and Multivariable Bioprocess Control. *IEEE Lat. Am. Trans.* **2021**, *19*, 798–806. [CrossRef]
21. Fernández, M.C.; Pantano, M.N.; Rodriguez, L.; Scaglia, G. State Estimation and Nonlinear Tracking Control Simulation Approach. Application to a Bioethanol Production System. *Bioprocess Biosyst. Eng.* **2021**, *44*, 1755–1768. [CrossRef] [PubMed]
22. López-Rodríguez, M.; Cerón-García, M.C.; López-Rosales, L.; Navarro-López, E.; Sánchez-Mirón, A.; Molina-Miras, A.; Abreu, A.C.; Fernández, I.; García-Camacho, F. Improved Extraction of Bioactive Compounds from Biomass of the Marine Dinoflagellate Microalga *Amphidinium Carterae*. *Bioresour. Technol.* **2020**, *313*, 123518. [CrossRef] [PubMed]
23. Richmond, A. *Handbook of Microalgal Culture: Biotechnology and Applied Phycology*, 1st ed.; Blackwell Science Ltd.: Oxford, UK, 2004; ISBN 0-632-05953-2.
24. Andersen, R. *Algal Culturing Techniques*; Elsevier: Amsterdam, The Netherlands, 2005; Volume 4, ISBN 0120884267.

25. OIV. *Compendium of International Methods of Wine and Must Analysis*; International Organisation of Vine and Wine: Dijon, France, 2021; ISBN 9782850380334.
26. Olivia, B.; Vega, A. Determinación de Peso Seco y Contenido Orgánico e Inorgánico. In *Métodos y Herramientas Analíticas en la Evaluación de la Biomasa Microalgal*; Centro de Investigaciones Biológicas del Noroeste: La Paz, Mexico, 2017.
27. Groff, M.C.; Scaglia, G.; Gaido, M.; Kassuha, D.; Ortiz, O.A.; Noriega, S.E. Kinetic Modeling of Fungal Biomass Growth and Lactic Acid Production in *Rhizopus Oryzae* Fermentation by Using Grape Stalk as a Solid Substrate. *Biocatal. Agric. Biotechnol.* **2022**, *39*, 102255. [CrossRef]
28. Cante, R.C.; Gallo, M.; Nigro, F.; Passannanti, F.; Budelli, A.; Nigro, R. Mathematical Modeling of *Lactobacillus Paracasei CBA L74* Growth during Rice Flour Fermentation Performed with and without pH Control. *Appl. Sci.* **2021**, *11*, 2921. [CrossRef]
29. Germec, M.; Turhan, I. Enhanced Production of *Aspergillus Niger* Inulinase from Sugar Beet Molasses and Its Kinetic Modeling. *Biotechnol. Lett.* **2020**, *42*, 1939–1955. [CrossRef] [PubMed]
30. Manthos, G.; Koutra, E.; Mastropetros, S.G.; Zagklis, D.; Kornaros, M. Mathematical Modeling of Microalgal Growth during Anaerobic Digestion Effluent Bioremediation. *Water* **2022**, *14*, 3938. [CrossRef]
31. Smith, H. *An Introduction to Delay Differential Equations with Applications to the Life Sciences*; Springer Science & Business Media: Berlin/Heidelberg, Germany, 2010; Volume 1, ISBN 978-1-4419-7645-1.
32. Groff, C.; Kuchen, B.; Gil, R.; Fernández, C. Scaglia Application of the Luedeking and Piret with Delay Time Model in Bioproductions with Non-Zero Kinetic Parameters. *IEEE Lat. Am. Trans.* **2023**, *21*, 882–888. [CrossRef]
33. James, G.; Witten, D.; Hastie, T.; Tibshirani, R.; Taylor, J. Linear Regression. In *An Introduction to Statistical Learning*; Springer: Berlin/Heidelberg, Germany, 2023.
34. Tempo, R.; Ishii, H. Monte Carlo and Las Vegas Randomized Algorithms for Systems and Conrol. *Eur. J. Control* **2007**, *13*, 189–203. [CrossRef]
35. Troncoso, C.; Suárez, A. Control Del Nivel de Pulpa En Un Circuito de Flotación Utilizando Una Estrategia de Control Predictivo. *Rev. Iberoam. De Automática E Informática Ind.* **2017**, *14*, 234–245. [CrossRef]
36. Aranda, A.; Matallana, E.; Del Olmo, M. *Saccharomyces Yeasts I: Primary Fermentation*; Academic Press: Cambridge, MA, USA, 2011; ISBN 9780123750211.
37. Ashour, M.; Mansour, A.T.; Alkhamis, Y.A.; Elshobary, M. Usage of *Chlorella* and Diverse Microalgae for CO_2 Capture-towards a Bioenergy Revolution. *Front. Bioeng. Biotechnol.* **2024**, *12*, 1387519. [CrossRef] [PubMed]
38. Prusova, B.; Humaj, J.; Kulhankova, M.; Kumsta, M.; Sochor, J.; Baron, M. Capture of Fermentation Gas from Fermentation of Grape Must. *Foods* **2023**, *12*, 574. [CrossRef] [PubMed]
39. Chunzhuk, E.A.; Grigorenko, A.V.; Kiseleva, S.V.; Chernova, N.I.; Ryndin, K.G.; Kumar, V.; Vlaskin, M.S. The Influence of Elevated CO_2 Concentrations on the Growth of Various Microalgae Strains. *Plants* **2023**, *12*, 2470. [CrossRef] [PubMed]
40. Liu, S.; Lou, Y.; Li, Y.; Zhao, Y.; Laaksonen, O.; Li, P.; Zhang, J.; Battino, M.; Yang, B.; Gu, Q. Aroma Characteristics of Volatile Compounds Brought by Variations in Microbes in Winemaking. *Food Chem.* **2023**, *420*, 136075. [CrossRef]
41. Ren, H.; Liu, B.; Ma, C.; Zhao, L.; Ren, N. A New Lipid-Rich Microalga *Scenedesmus* sp. Strain R-16 Isolated Using Nile Red Staining: Effects of Carbon and Nitrogen Sources and Initial PH on the Biomass and Lipid Production. *Biotechnol. Biofuels* **2013**, *6*, 143. [CrossRef]
42. Turon, V.; Baroukh, C.; Trably, E.; Latrille, E.; Fouilland, E.; Steyer, J.P. Use of Fermentative Metabolites for Heterotrophic Microalgae Growth: Yields and Kinetics. *Bioresour. Technol.* **2015**, *175*, 342–349. [CrossRef] [PubMed]
43. Yeh, K.L.; Chen, C.Y.; Chang, J.S. PH-Stat Photoheterotrophic Cultivation of Indigenous *Chlorella Vulgaris* ESP-31 for Biomass and Lipid Production Using Acetic Acid as the Carbon Source. *Biochem. Eng. J.* **2012**, *64*, 1–7. [CrossRef]
44. Prasad, R.; Gupta, S.K.; Shabnam, N.; Oliveira, C.Y.B.; Nema, A.K.; Ansari, F.A.; Bux, F. Role of Microalgae in Global CO_2 Sequestration: Physiological Mechanism, Recent Development, Challenges, and Future Prospective. *Sustainability* **2021**, *13*, 13061. [CrossRef]
45. Minillo, A.; Godoy, H.C.; Fonseca, G.G. Growth Performance of Microalgae Exposed to CO_2. *J. Clean Energy Technol.* **2013**, *1*, 110–114. [CrossRef]
46. Pourjamshidian, R.; Abolghasemi, H.; Esmaili, M.; Amrei, H.D.; Parsa, M.; Rezaei, S. Carbon Dioxide Biofixation by *Chlorella* sp. in a Bubble Column Reactor at Different Flow Rates and CO_2 Concentrations. *Braz. J. Chem. Eng.* **2019**, *36*, 639–645. [CrossRef]
47. Politaeva, N.; Ilin, I.; Velmozhina, K.; Shinkevich, P. Carbon Dioxide Utilization Using *Chlorella* Microalgae. *Environments* **2023**, *10*, 109. [CrossRef]
48. Mora-Godínez, S.; Rodríguez-López, C.E.; Senés-Guerrero, C.; Treviño, V.; Díaz De La Garza, R.; Pacheco, A. Effect of High CO_2 Concentrations on *Desmodesmus abundans* RSM Lipidome. *J. CO2 Util.* **2022**, *65*, 102183. [CrossRef]
49. LAFFORT Medida De La Concentración De Azúcares En Mosto. Available online: https://laffort.com/wp-content/uploads/Protocols/ES_Table_Convertisseur.pdf (accessed on 18 December 2024).
50. Eze, V.C.; Velasquez-Orta, S.B.; Hernández-García, A.; Monje-Ramírez, I.; Orta-Ledesma, M.T. Kinetic Modelling of Microalgae Cultivation for Wastewater Treatment and Carbon Dioxide Sequestration. *Algal Res.* **2018**, *32*, 131–141. [CrossRef]

51. Shetty, P.; Gitau, M.M.; Maróti, G. Salinity Stress Responses and Adaptation Mechanisms in Eukaryotic Green Microalgae. *Cells* **2019**, *8*, 1657. [CrossRef]
52. Abinandan, S.; Praveen, K.; Venkateswarlu, K.; Megharaj, M. Eco-Innovation Minimizes the Carbon Footprint of Wine Production. *Commun. Earth Environ.* **2024**, *5*, 618. [CrossRef]
53. Spennati, E.; Casazza, A.A.; Converti, A.; Busca, G. Investigation on Thermal Pyrolysis of Microalgae Grown in Winery Wastewater: Biofuels and Chemicals Production. *Biomass Convers. Biorefinery* **2024**, *14*, 17647–17661. [CrossRef]
54. Spennati, E.; Casazza, A.A.; Converti, A.; Padula, M.P.; Dehghani, F.; Perego, P.; Valtchev, P. Winery Waste Valorisation as Microalgae Culture Medium: A Step Forward for Food Circular Economy. *Sep. Purif. Technol.* **2022**, *293*, 121088. [CrossRef]
55. Zkeri, E.; Mastori, M.; Xenaki, A.; Kritikou, E.; Kostakis, M.; Dasenaki, M.; Maragou, N.; Fountoulakis, M.; Thomaidis, N.; Stasinakis, A. Winery Wastewater Treatment by Microalgae *Chlorella Sorokiniana* and Characterization of the Produced Biomass for Value-Added Products. *Environ. Sci. Pollut. Res.* **2024**, *36*, 49244–49254. [CrossRef] [PubMed]
56. Praveen, K.; Abinandan, S.; Venkateswarlu, K.; Megharaj, M. Emergy Analysis and Life Cycle Assessment for Evaluating the Sustainability of Solar-Integrated Ecotechnologies in Winery Wastewater Treatment. *ACS Sustain. Chem. Eng.* **2024**, *12*, 4676–4689. [CrossRef]